Kidney International, Vol. 64 (2003), pp. 2079–2091

DNA oligonucleotide microarray technology identifies fisp-12 among other potential fibrogenic genes following murine unilateral ureteral obstruction (UUO): Modulation during epithelial-mesenchymal transition

Debra F. Higgins, David W.P. Lappin, Niamh E. Kieran, Hans J. Anders, Ronald W.G. Watson, Frank Strutz, Detlef Schlondorff, Volker H. Haase, John M. Fitzpatrick, Catherine Godson, and Hugh R. Brady

Department of Medicine and Therapeutics, University College Dublin, Dublin, Ireland; Department of Surgery, Mater Misericordiae Hospital, Dublin, Ireland; Conway Institute of Biomolecular and Biomedical Research, Dublin, Ireland; Dublin Molecular Medicine Centre, Dublin, Ireland; Department of Nephrology and Rheumatology, Georg-August University Medical Centre, Gottingen, Germany; Nephrological Centre, Ludwig Maximilians University, Munich, Germany; and Department of Medicine, University of Pennsylvania, Philadelphia, Pennsylvania

DNA oligonucleotide microarray technology identifies fisp-12 among other potential fibrogenic genes following murine unilateral ureteral obstruction (UUO): Modulation during epithelial-mesenchymal transition.

Background. Tubulointerstitial inflammation and fibrosis are pathologic hallmarks of end-stage renal disease (ESRD). Here we have used DNA microarray technology to monitor the transcriptomic responses to murine unilateral ureteral obstruction (UUO) with a view to identifying molecular modulators of tubulointerstitial fibrosis.

Methods. Using Affymetrix Mu74Av2 microarrays, gene expression 4 and 10 days postobstruction was investigated relative to control contralateral kidneys. Candidate profibrogenic genes were further investigated in epithelial cells undergoing epithelial to mesenchymal transition (EMT) in vitro.

Results. mRNA levels for 1091 gene/EST sequences, of a total of 12,488 displayed on the microarray, were altered twofold or greater by days 4 and 10 postobstruction compared to contralateral control kidneys. Genes were categorised into functional groups, including modulators of cytoskeletal and extracellular matrix metabolism, cell growth, signalling, and transcription/translational events. Among the potentially profibrogenic genes, whose mRNA levels were increased after UUO, were fibroblast-inducible secreted protein (fisp-12), the murine homologue of connective tissue growth factor (CTGF), collagen XVIIIα1, secreted protein acidic and rich in cysteine (SPARC), and src-suppressed C-kinase substrate (SSeCKS). A sustained increase in fisp-12 mRNA level was observed during EMT induced by transforming growth factor-β1 (TGF-β1) and epidermal growth factor (EGF).

Conclusion. Altered gene expression in murine UUO has been demonstrated. Increased expression of fisp-12, SPARC, and SSeCKS has been shown in response to TGF-β1 treatment and during EMT, suggesting that these genes may offer potential therapeutic targets against tubulointerstitial fibrosis.

Key words: renal fibrosis, UUO, microarray analysis, profibrogenic genes, fisp-12, collagen XVIIIα1, SPARC, SSeCKS.

Received for publication August 22, 2002
and in revised form May 1, 2003, and June 19, 2003
Accepted for publication July 14, 2003

Tubulointerstitial inflammation and fibrosis are pathologic hallmarks of end-stage renal disease (ESRD). Renal tubulointerstitial fibrosis develops regardless of the initiating insult and the extent of fibrosis correlates with the loss of renal function [1, 2]. Chronic unilateral ureteral obstruction (UUO) is a well-characterized model of tubulointerstitial fibrosis [3] and promotes interstitial extracellular matrix accumulation with tubular epithelial cell atrophy and apoptosis [4]. Pathologic roles for transforming growth factor-β1 (TGF-β1) [5], vascular cell adhesion molecule-1 (VCAM-1) [6], intercellular adhesion molecule-1 (ICAM-1) [6, 7], heat shock protein 47 (HSP47) [8], and Smad 7 [9] among other mediators of tubulointerstitial damage have been demonstrated using this model. We have exploited this in vivo model to investigate the transcriptomic responses implicated in the pathology of renal fibrosis by oligonucleotide microarrays.

During UUO, a number of changes occur in the obstructed kidney that culminate in the progression of tubulointerstitial fibrosis. In the mouse UUO model, increased numbers of inflammatory cells are observed in the tubulointerstitium as early as day 4, tubular epithelial cells initially proliferate and then undergo apoptosis

leading to loss of epithelial integrity [4]. Tubular lumens undergo dilatation and tubular epithelial cells become flattened. Increased numbers of fibroblasts are observed in the interstitium, which are postulated to derive from (*1*) proliferation of resident fibroblast populations, (*2*) recruitment of fibrocytes from the circulation, and (*3*) transition of tubular epithelial cells toward a fibroblast phenotype. Extracellular matrix molecules accumulate in the interstitial compartment and by day 10 postobstruction the degree of fibrosis in the murine kidney is extensive. In the present study, Affymetrix Mu74Av2 arrays, representing over 12,000 murine sequences, were employed to analyze gene expression at days 4 and 10 postobstruction. Day 4 post-UUO was chosen to represent an early time point in the development of tubulointerstitial fibrosis where changes in inflammatory genes and associated growth factor populations would be detected. Day 10 post-UUO, dominated by fibrotic tissue, was studied to identify genes whose expression remains altered in a fibrotic environment. We predicted that over the course of ureteral ligation, we would observe an increase in profibrotic genes, a decrease in epithelial cell growth regulators, an increase in proinflammatory and apoptosis-related genes, and potentially a change in gene expression corresponding to epithelial-mesenchymal transition (EMT) and myofibroblastic proliferation.

Gene expression in UUO kidneys was compared to that of contralateral unobstructed kidneys. Although contralateral kidneys respond to UUO of the ipsilateral kidney by increasing glomerular filtration rates, changes observed in the gene expression of the contralateral kidney more closely parallel that of age-matched control sham-operated kidneys [10, 11]. Indeed, tubular and interstitial cell proliferation and apoptotic rates in the contralateral kidney are similar to that of sham-operated control kidneys [12]. Furthermore, contralateral kidneys at day 10 postobstruction do not display any histomorphologic damage [13]. Therefore, in our experiments, baseline gene expression was taken as the expression level observed in the contralateral kidney.

Transcripts differentially expressed in obstructed kidneys included (*1*) genes whose expression had been reported previously in UUO and tubulointerstitial fibrosis and which serve to validate the approach, (*2*) genes not implicated in the pathogenesis of tubulointerstitial fibrosis heretofore, but whose profile of biologic activity elsewhere suggests a novel role, and (*3*) unannotated genes.

Among the genes up-regulated in response to UUO was fibroblast-inducible secreted protein (fisp-12), the murine homologue of human connective tissue growth factor (CTGF) [14]. Recent evidence suggests that this gene may play an important role in the development of tubulointerstitial fibrosis [15]. We have further examined the expression of this gene in proximal tubular epithelial cells in vitro in response to TGF-β1 stimulation, which induces EMT, a process that recently has been determined to contribute significantly to renal fibrosis [16]. CTGF has been recognized as a down-stream mediator of TGF-β1 signaling [17] and has been shown to induce collagen deposition in several renal cell lines, including mesangial cells and interstitial fibroblasts. Here, we report the production of CTGF by proximal tubular epithelial cells, further highlighting the pathophysiologic potential of this gene in renal fibrosis.

Cytokines and growth factors are important stimuli for renal fibrosis due to EMT within diseased kidneys [18] and approximately one third of fibroblasts in fibrotic kidneys appear to be derived from EMT of tubular epithelial cells [16]. During EMT, tubular cells lose their epithelial cell markers, including cytokeratin, and express increased levels of fibroblast markers, including vimentin, and fibroblast-specific protein 1 (fsp-1) [19]. Collagen I deposition has been associated with myofibroblast cells in areas of tubulointerstitial fibrosis, and the origin of these myofibroblasts has been linked to transition of tubular epithelial cells [18–20]. In order to further investigate the role of EMT in tubulointerstitial fibrosis, we performed in vitro studies on proximal tubular epithelial cells stimulated with TGF-β1. Interestingly, we found that a number of the genes identified in our microarray screen were also responsive to TGF-β1 treatment, highlighting the importance of this growth factor in the progression of fibrosis. We further analyzed the expression of secreted protein acidic and rich in cysteine (SPARC), src-suppressed C-kinase substrate (SSeCKS), and collagen XVIIIα1 during EMT since these were identified in our microarray screens and are suggested in the literature to play a role in the control of cytoskeletal structure, which undergoes marked changes during the EMT process.

In summary, this report details our findings of global gene expression changes occurring during the development of tubulointerstitial fibrosis. Our screen identified over 1000 genes whose expression was altered in response to UUO and involved the identification of genes already associated with fibrosis along with novel associations. Of the genes identified, we further analyzed fisp-12 (CTGF), collagen XVIIIα1, SSeCKS, and SPARC expression in vitro in response to TGF-β1 stimulation and have shown that these genes act downstream of this cytokine and therefore may play important roles in the progression of renal fibrosis. Our microarray data, available online at *http://www.ucd.ie/conway/*offers valuable information into the changes which occur in gene expression during the process of tubulointerstitial fibrosis.

METHODS

Unilateral ureteral obstruction

Obstructed ($N = 4$ day 4, $N = 4$ day 10) and contralateral control kidneys ($N = 4$ day 4, $N = 4$ day 10) were

prepared as follows. C57BL/6 mice of 12 ± 2 weeks of age were kept in macrolone type III cages under a 12-hour light and dark cycle, water and standard chow (Sniff, Soest, Germany) were available ad libitum. Ureteric obstruction was performed under general anesthesia by ligating the left ureter with 4-0 mersilene through a midline abdominal incision [13]. Mice were sacrificed either 4 days or 10 days post-UUO by cervical dislocation under general anesthesia with inhaled ether. Contralateral kidneys were used as intraindividual nonobstructed controls. Histologic examination of the obstructed kidneys revealed a macrophage and lymphocytic cell infiltrate in the tubulointerstitium, interstitial fibrosis, tubular dilation, and tubular cell flattening with necrosis/apoptosis progressing from day 4 to day 10. All animal experiments were carried out in accordance with the ethical guidelines of the Ludwig Maximilians University.

Cell culture and EMT

Murine proximal tubular (MCT) epithelial cells [21] were grown in Dulbecco's modified Eagle's medium (DMEM)/Ham's F12 medium (Invitrogen, Carlsbad, CA, USA) supplemented with 10% fetal calf serum (FCS), 1% glutamine, 1% penicillin, and 1% streptomycin. For experiments, cells were serum starved in K-1 medium: DMEM/Ham's F12 medium supplemented with 1% glutamine, 1% penicillin, and 1% streptomycin, 5 μg/mL insulin, 5 μg/mL transferrin, 5 ng/mL selenium, and 36 ng/mL hydrocortisone [18]. To investigate the potential of TGF-β1 to drive the expression of fisp-12, 5×10^4 MCT cells were plated onto 6-well plates (Costar Cambridge, MA, USA), grown for 48 hours at 37°C in the presence of 5% CO_2, serum starved for 24 hours and treated with either 3 or 10 ng/mL TGF-β1 for 24 hours. MCT cells were induced to undergo EMT according to the protocol of Strutz et al [19] using 3 ng/mL TGF-β1 and 10 ng/mL EGF for 72 hours.

RNA isolation and semiquantitiative reverse transcription-polymerase chain reaction (RT-PCR)

Total RNA was extracted from obstructed and contralateral murine kidneys and MCT epithelial cells using TRizol® LS reagent (Invitrogen) as per manufacturer's instructions. Two micrograms total RNA was DNase-treated with 1 U DNase I (Invitrogen) for 15 minutes at room temperature in a 10 μL reaction. The DNase was inactivated by the addition of 1 μL of 25 mmol/L ethylenediaminetetraacetic acid (EDTA) at 65°C for 10 minutes. DNase-treated total RNA was reverse-transcribed in a 20 μL reaction containing 50 mmol/L Tris-HCl, pH 8.3, 75 mmol/L KCl, 3 mmol/L $MgCl_2$, 10 mmol/L dithiothreitol (DTT), 500 μmol/L desoxynucleoside triphosphate (dNTP), 100 ng of random hexamers (Invitrogen). Two hundred units of Superscript II RNase H^- reverse transcriptase were added and the reactions incubated at 42°C for 1 hour. One microliter of each RT reaction was PCR amplified in a 50 μL reaction containing 20 mmol/L Tris-HCl, pH 8.4, 50 mmol/L KCl, 1.5 mmol/L $MgCl_2$, 200 mmol/L dNTP, and 100 ng of forward (F) and reverse (R) primers: epidermal growth factor (EGF)-F, 5′-CGG AAG TAC TGC GAA GAT GTC, EGF-R, 5′-TAG ATT CTC CGG CCA ATC CA, 658 bp product; ColIα1-F, 5′-ATG TTC AGC TTT GTG GAC CTC CG, ColIα1-R, 5′-TCA TAG CCA TAG GAC ATC TGG G, 473 bp product; transgelin-F, 5′-CTG AGC AAR TTG GTG AAC AGC, transgelin-R, 5′-CCA TGT GCA GTC ATC TTT GC, 541 bp product; fisp12-F, 5′-CTA AGA CCT GTG GAA TGG GC, fisp12-R, 5′-CTC AAA GAT GTC ATT GTC CCC, 386 bp product; Col8α1-F, 5′-AYT TCC CAG TGC TTC CAG CAA G, Col8α1-R, 5′-TTG GAG AAA GAG GTC ATG AAG C, 460 bp product; fsp1-F, 5′-CCA CCT TCC ACA ART ACT CRG G, fsp1-R, 5′-TCW GAG GAG TYT TCA YTT CTT CC, 470 bp product; SPARC-F, 5′-GCA ATG ACA ACA AGA CCT TCG, SPARC-R, 5′-TTG TCS TTG TCT AGG TCA CAG G, 498 bp product; SSeCKS-F, 5′-TGA AGC AAT CCA CAG AGA AGC, SSeCKS-R, 5′-CTC ATC AAA CAC TTC CGT TGC, 499 bp product; glyceraldehyde-3-phosphate dehydrogenase (GAPDH)-F, 5′-ACC ACA GTC CAT GCC ATC, GAPDH-R, 5′-TCC ACC ACC CTG TTG CTG, 452 bp product; 18S-F, GTG GAG CGA TTT GTC TGG TT and 18S-R, CGC TGA GCC AGT CAG TGT AG, 200 bp product. PCR amplification was typically performed at 25 to 30 cycles of 94°C, 57°C, and 72°C for 30 seconds each followed by a final 3-minute extension at 72°C. RT-PCR products were resolved on 1% agarose gels and visualized by ethidium bromide staining. All samples were quantitated using image software Grabit and Gelworks (Ultra-Violet Products, Cambridge, UK) and were normalized to their respective 18S rRNA products.

Quantitative real-time PCR

Two micrograms of total RNA was reverse-transcribed using random hexamers as described above. Quantitative real-time PCR was performed using TaqMan universal PCR master mix (P/N 4304437, Applied Biosystems, Weiterstadt, Germany) as per manufacturer's protocol. Samples were run in duplicate and were analyzed using the ABI Prism 7700 Sequence Detection System (Applied Biosystems). Probes, labeled with FAM, and primers were designed using Primer Express (Applied Biosystems): TGF-β1 probe, AGC GCA TCG AAG CCA TCC GTG, TGF-β1 forward, TCG ACA TGG AGC TGG TGA AA, TGF-β1 reverse, TGG CGA GCC TTA GTT TGG A; fisp-12 probe, CCC CCG CCA ACC GCA AGA TT, fisp-12 forward, CCC ACA CAA GGG CCT CTT C, fisp-12 reverse, CCA TCT TTG GCA GTG

CAC AC. TaqMan PCR reactions were multiplexed for the gene of interest and VIC- labeled 18S rRNA, as an endogenous control (P/N 4310893E, Applied Biosystems).

Affymetrix oligonucleotide microarray analysis

Total RNA was isolated from obstructed and contralateral kidneys ($N = 4$ for treated and control at each time point) and purified through an RNeasy minicolumn (Qiagen, Valencia, CA, USA). Five micrograms of RNA from each treatment were pooled. Five micrograms of the pooled RNA was reverse-transcribed as above in a 20 μL reaction. Second-strand cDNA was synthesized by adding 1× second-strand buffer [20 mmol/L Tris-HCl, pH 6.9, 4.6 mmol/L $MgCl_2$, 90 mmol/L KCl, 150 mmol/L β-NAD^+, and 10 mmol/L $(NH_4)_2SO_4$ final concentration], 200 mmol/L dNTP, 10 U DNA Ligase, 40 U DNA polymerase I, and 2 U RNase H to the first-strand reaction to a final volume of 150 μL. Samples were incubated at 16°C for 2 hours. Ten units T_4 DNA polymerase was added at 16°C for 5 minutes followed by 10 μL of 0.5 mol/L EDTA. The double-stranded cDNA was phenol-chloroform extracted and precipitated with 0.75 volumes of 5 mol/L NH_4OH acetate and 2.5 volumes of ice-cold absolute ethanol. The cDNA was pelleted at 12,000 × *g* for 20 minutes at 4°C, washed twice with 500 μL of ice-cold 75% ethanol in diethyl pyrocarbonate (DEPC)-treated water and resuspended in 12 μL of DEPC water. Ten microliters of double-stranded cDNA was used as a template for the production of biotin-labeled cRNA using the Bioarray High-Yield RNA Transcript Labeling Kit (Enzo, Farmingdale, NY, USA) as per manufacturer's instructions. cRNA was fragmented in 1× fragmentation buffer (40 mmol/L Tris-acetate, pH 8.1, 100 mmol/L KO acetate, 30 mmol/L MgO acetate) at 94°C for 35 minutes. Fifteen micrograms of fragmented cRNA was hybridized to the Mu74Av2 array as per Affymetrix protocol. Arrays were washed and fluorescently labeled prior to scanning with a confocal scanner (Affymetrix). cRNA from freshly pooled RNA was prepared as above and hybridized to a second set of arrays (as duplicate experiments). Affymetrix Microarray Suite 5.0 was used to scan and analyze the arrays, expression analysis was performed using this software. Criteria for the selection of genes included (*1*) presence on duplicate oligonucleotide microarrays (with a similar Affymetrix flag call on straight and cross-comparisons of the duplicate arrays of treated kidneys to respective controls) and (*2*) those which displayed a greater than twofold average change in expression for at least one of the time points [an average for the straight and cross comparisons of the duplicate arrays (i.e., four comparisons for each time point) was calculated]. Microarray data in tables are shown as mean signal log ratio (where 1 is equivalent to a twofold change in expression) ± standard deviation from the mean.

Statistical analysis

Data for gene chip analysis are expressed as mean ± standard deviation. For the RT and the real time-PCR analysis, data are expressed as mean ± SEM. Statistical analysis was performed using a Student *t* test, a *P* value <0.05 was considered statistically significant.

RESULTS

Increased mRNA levels for fisp-12, among other profibrotic genes, following UUO as identified by oligonucleotide microarrays

Alterations of gene expression in response to UUO were analyzed using the Affymetrix Mu74Av2 oligonucleotide microarray, representing approximately 6000 known gene sequences and 6000 EST sequences. Genes were compared and selected as described in the **Methods** section, using duplicate arrays each analyzing mRNA pooled from four individual animals and using a twofold change in gene expression as a cutoff point (signal log ratio of 1 is equivalent to twofold up-regulation in gene expression, −1 equivalent to a twofold down-regulation, and 0 equivalent to no change). A total of 1091 gene/EST sequences passed the selection criteria. Of these sequences, 606 (55.5%) were up-regulated, 430 of which represented annotated genes with the remainder representing ESTs, and 485 (44.5%) were down-regulated sequences, 251 representing annotated genes.

Murine kidneys subjected to UUO for 4 days ($N = 4$) or 10 days ($N = 4$) were compared to their respective unobstructed contralateral kidneys as control ($N = 4$ at each time point). Genes differentially expressed in response to UUO included those encoding extracellular matrix and cytoskeletal molecules (64 induced and seven repressed), cell growth and differentiation related-molecules (47 induced and five repressed), cytokines and growth factors (35 induced and seven repressed) (see Tables 1 to 3), signaling molecules (58 induced and 17 repressed), and those involved with mRNA expression and translation (51 induced and 13 repressed). A complete list of gene expression findings is available for download at *http://www.ucd.ie/conway/*

Genes were analyzed on the basis of their temporal expression pattern. Interestingly, the majority of genes, which were differentially regulated in response to UUO by day 4, were further increased or decreased by day 10 (Table 1). A small number of genes were identified that showed a change in expression level by day 4 but displayed a "no change" call by day 10 postobstruction (Table 2). Furthermore, we identified a small number of genes that displayed a "no change" call by day 4 postobstruction but were either up- or down-regulated by day 10 (Table 3). Of note, this group included plasminogen activator inhibitor (PAI-1), which has been shown

Table 1. Genes whose expression is altered at both days 4 and 10 post unilateral ureteral obstruction (UUO)

GenBank ID	Gene family	Mean signal log ratio[a] Day 4 ± SD	Day 10 ± SD
	Extracellular matrix and cytoskeletal		
X66405	Procollagen, type VI, alpha 1	0.33 ± 0.24	1.05 ± 0.07
U03184	Cortactin	0.38 ± 0.40	1.25 ± 0.49
M63801	Connexin 43 (alpha-1 gap junction)	0.50 ± 0.37	1.60 ± 0.57
X98475	VASP gene	0.58 ± 0.05	1.20 ± 0.57
AF022432	MMP-14	0.58 ± 0.13	1.45 ± 0.21
L00923	Myosin I	0.58 ± 0.19	1.45 ± 0.49
D14340	Tight junction protein 1	0.65 ± 0.17	1.00 ± 0.28
U43327	Laminin, gamma 2	0.65 ± 0.10	1.50 ± 0.28
M13441	Alpha-tubulin isotype M-alpha-6	0.68 ± 0.10	1.05 ± 0.07
L23769	Microfibril-associated glycoprotein	0.68 ± 0.35	1.15 ± 0.21
M28727	Tubulin alpha 2	0.73 ± 0.13	1.00 ± 0.14
M84683	Tumor-associated mucin 1	0.75 ± 0.13	1.30 ± 0.00
U66166	Extracellular matrix protein 2	0.93 ± 0.28	2.00 ± 0.00
Y11460	Beta 4 integrin interactor, partial	0.98 ± 0.10	1.00 ± 0.14
M28729	Tubulin alpha 1	1.00 ± 0.24	1.85 ± 0.07
M28739	Tubulin, beta 2	1.03 ± 0.10	0.90 ± 0.00
D17546	Procollagen, type XV	1.05 ± 0.19	1.30 ± 0.00
X04647	Procollagen, type IV, alpha 2	1.05 ± 0.17	1.55 ± 0.21
M28729	Tubulin alpha 1	1.08 ± 0.05	1.20 ± 0.00
L17324	Nidogen	1.08 ± 0.15	1.40 ± 0.14
X15662	Cytokeratin endo A	1.23 ± 0.10	1.65 ± 0.07
X04663	Beta-tubulin (isotype M beta 5)	1.23 ± 0.44	1.85 ± 0.21
X56304	Tenascin C	1.23 ± 0.40	2.15 ± 0.35
J03520	Plasminogen activator, tissue	1.25 ± 0.17	1.30 ± 0.28
X60676	HSP47	1.33 ± 0.15	1.75 ± 0.07
X04663	Beta-tubulin (isotype M beta 5)	1.35 ± 0.10	2.05 ± 0.07
AI853217[b]	Vascular epithelium cadherin	1.40 ± 0.64	1.20 ± 0.28
U04354	ADSEVERIN	1.40 ± 0.32	1.65 ± 0.07
X52490	$Beta_2$ microglobulin	1.45 ± 0.13	1.55 ± 0.07
X01838	$Beta_2$ microglobulin	1.55 ± 0.13	0.70 ± 0.00
X13297	Vascular smooth muscle alpha-actin	1.55 ± 0.37	1.80 ± 0.00
Z68618	Trasngelin	1.60 ± 0.12	1.75 ± 0.21
L02918	Procollagen type V alpha 2 (Col5a-2)	1.60 ± 0.54	2.00 ± 0.28
M22479	Tropomyosin isoform 2	1.60 ± 0.26	2.00 ± 0.00
Z19543	h2-calponin cDNA	1.65 ± 0.45	1.65 ± 0.21
M22832	Cytokeratin endoB	1.68 ± 0.38	2.25 ± 0.21
X04017	Cysteine-rich glycoprotein SPARC	1.75 ± 0.13	2.30 ± 0.14
X54511	Myc basic motif homologue-1, mbh1	1.78 ± 0.10	1.35 ± 0.07
U72519	Ena-VASP like protein (Evl)	1.80 ± 1.16	2.15 ± 0.07
AB000713	mCPE-R CPE-receptor	1.83 ± 0.73	2.40 ± 0.14
U38967	Prothymosin beta 4	1.80 ± 0.18	1.90 ± 0.14
M15832	Procollagen, type IV, alpha 1	1.93 ± 0.37	1.55 ± 0.35
AA763466[b]	Collagen, alpha 1 type 1	1.93 ± 0.10	2.10 ± 0.28
L22545	Procollagen, type XVIII, alpha 1	2.00 ± 0.08	1.55 ± 0.07
U03715	Procollagen, type XVIII, alpha 1	2.25 ± 0.17	1.80 ± 0.28
L29454	Fibrillin 1	2.28 ± 0.72	2.30 ± 1.13
X58251	Procollagen, type I, alpha 2	2.28 ± 0.22	3.10 ± 0.14
AF064749	Type VI collagen alpha 3 subunit	2.68 ± 0.94	2.40 ± 0.14
AF011450	Procollagen, type XV	2.73 ± 0.21	2.30 ± 0.00
AV234303*	Collagen, alpha 1 type III	2.78 ± 0.77	4.00 ± 0.14
AB020886	SSeCKS	2.88 ± 1.31	2.90 ± 0.42
X52046	Procollagen, type III, alpha 1	2.88 ± 0.38	3.65 ± 0.07
M36120	Keratin complex 1, acidic, gene 19	2.90 ± 0.16	6.00 ± 1.41
U03419	Alpha-1 type I procollagen	3.20 ± 0.16	3.70 ± 0.00
D49691	p50b (identical to LSP 1 and pp52)	4.10 ± 0.57	3.15 ± 0.78
M81445	Gap junction membrane channel protein beta 2	−0.70 ± 0.22	−1.95 ± 0.07
M18775	Microtubule-associated protein tau	−0.60 ± 0.41	−1.70 ± 0.57
M18775	Microtubule-associated protein tau	−0.55 ± 0.25	−1.30 ± 0.28
U26437	Tissue inhibitor of metalloproteinases-3 (TIMP-3)	−0.55 ± 0.13	−1.20 ± 0.14
D78646	Zeta-crystallin	−0.45 ± 0.06	−1.20 ± 0.14
L40632	Ankyrin 3, epithelial	−0.38 ± 0.34	−1.00 ± 0.14
	Cell growth and differentiation		
U44088	TDAG51 (TDAG51)	0.45 ± 0.24	1.10 ± 0.28
L01640	D-type G1 cyclin catalytic subunit, PSK-J3	0.63 ± 0.05	1.00 ± 0.14
AF035939	Mago-nashi homolog	0.70 ± 0.22	1.00 ± 0.14
AF027707	Apoptosis activator Mtd (Mtd)	0.70 ± 0.36	1.20 ± 0.42
M73748	OTS-8	0.70 ± 0.18	2.25 ± 0.21
U96635	Developmentally down-regulated gene 4	0.75 ± 0.13	1.10 ± 0.14
U60530	MAD homolog 2, (Drosophila)	0.75 ± 0.33	1.30 ± 0.14
X65687	Thymoma viral proto-oncogene	0.78 ± 0.13	1.00 ± 0.00

Table 1. (Continued)

GenBank ID	Gene family	Mean signal log ratio[a] Day 4 ± SD	Day 10 ± SD
J04103	E26 avian leukemia oncogene 2, 3 domain	0.80 ± 0.26	1.00 ± 0.00
X56602	Interferon-induced 15-kD protein	0.88 ± 0.43	2.10 ± 1.27
AJ001616	Myeloid associated differentiation protein	0.90 ± 0.18	1.15 ± 0.21
V00755	Interferon beta, fibroblast	0.90 ± 0.27	1.35 ± 0.21
V00727	FBJ osteosarcoma oncogene	0.93 ± 0.50	2.55 ± 2.47
X57796	Tumor necrosis factor receptor 1α	1.00 ± 0.12	0.90 ± 0.14
AJ223782	CDC10	1.08 ± 0.30	1.30 ± 0.28
AB021961	Mutant p53	1.10 ± 0.58	1.00 ± 0.21
U58992	MAD homolog 1 (Drosophila)	1.13 ± 0.25	1.30 ± 0.35
D78354	TRA1	1.15 ± 0.19	0.70 ± 0.14
Z16410	btg1	1.30 ± 0.18	1.15 ± 0.07
U00937	GADD45 protein (gadd45) gene	1.30 ± 0.18	1.45 ± 0.21
M21065	Interferon regulatory factor 1	1.45 ± 0.86	1.15 ± 0.07
U92565	Small inducible cytokine subfamily D, 1	1.45 ± 0.10	1.65 ± 0.07
U88909	Apoptosis inhibitor 2	1.53 ± 0.15	1.15 ± 0.07
X78989	Testin	1.55 ± 0.13	1.45 ± 0.07
D87661	14-3-3 eta	1.60 ± 0.08	1.25 ± 0.07
U15635	IFN-gamma induced (Mg11)	1.60 ± 0.42	2.55 ± 1.20
M21019	Harvey rat sarcoma oncogene, subgroup R	1.63 ± 0.73	1.55 ± 0.49
M28233	Interferon-gamma receptor	1.78 ± 0.67	1.45 ± 0.64
AB015978	Oncostatin receptor	1.78 ± 0.22	2.55 ± 0.07
AF058798	14-3-3 protein sigma	1.93 ± 0.85	2.50 ± 0.14
AB007599	MD-1	2.33 ± 0.26	2.80 ± 0.42
AA790307*	Onzin	2.48 ± 0.17	2.45 ± 0.07
AJ007970	mGBP-2 protein	2.58 ± 0.21	2.60 ± 0.00
U43085	Interferon-induced, tetratricopeptide repeats 2	2.75 ± 1.28	2.30 ± 0.57
L00039	Myelocytomatosis oncogene	2.83 ± 1.14	2.65 ± 0.78
U49513	Small inducible cytokine A9	3.30 ± 1.33	3.25 ± 0.92
J04596	GRO1 oncogene	4.25 ± 0.44	4.10 ± 0.28
X81627	24p3 gene	4.45 ± 0.47	5.75 ± 0.21
J04596	GRO1 oncogene	4.55 ± 0.90	3.65 ± 1.34
M19681	Small inducible cytokine A2	5.28 ± 0.63	4.85 ± 1.06
M21828	Growth arrest specific 2	−0.88 ± 0.10	−1.70 ± 0.00
AF100927	Apoptosis-inducing factor AIF	−0.78 ± 0.13	−1.25 ± 0.21
AF041377	Cell death activator CIDE-B	−0.65 ± 0.10	−1.40 ± 0.00
M31680	Growth hormone receptor	−0.65 ± 0.78	−1.35 ± 0.64
U18869	Mitogen-responsive 96 kDa phosphoprotein p96	−0.50 ± 0.08	−1.05 ± 0.07
	Cytokine and growth factor		
M29464	Platelet derived growth factor, alpha	0.55 ± 0.06	1.10 ± 0.14
D16195	Granulin	0.73 ± 0.05	1.10 ± 0.14
X04367	Platelet derived growth factor receptor, beta	0.78 ± 0.22	1.30 ± 0.42
AF020185	Protein inhibitor of nitric oxide synthase (PIN)	0.95 ± 0.13	1.00 ± 0.00
M70642	Fibroblast inducible secreted protein (fisp-12)	1.10 ± 0.24	1.45 ± 0.07
M59821	Growth factor-inducible protein (pip92)	1.10 ± 0.23	1.75 ± 0.07
AF099973	Schlafen2 (Slfn2)	1.15 ± 0.47	1.45 ± 0.07
L03529	Thrombin receptor	1.18 ± 0.49	1.35 ± 0.21
M28845	Early growth response 1	1.18 ± 1.09	1.65 ± 0.07
U90123	Hematological and neurological expressed 1	1.28 ± 0.74	1.50 ± 0.00
U23778	Hematopoietic-specific early-response A1-b	1.38 ± 0.28	2.75 ± 0.35
U41341	Endothelial monocyte-activating polypeptide I	1.48 ± 0.13	1.45 ± 0.07
M27960	Interleukin-4 receptor (secreted form)	1.58 ± 1.26	1.70 ± 0.57
U23781	Hematopoietic-specific early-response A1-d	1.58 ± 0.25	2.25 ± 0.07
L19932	TGF, beta induced, 68 kDa	1.60 ± 0.68	1.75 ± 0.07
M32490	Insulin-like growth factor binding protein 10	1.60 ± 0.36	1.95 ± 0.35
X62940	TGF beta 1 induced transcript 4	1.63 ± 0.10	1.65 ± 0.07
M91380	Follistatin-like	1.75 ± 0.42	2.15 ± 0.21
AF099973	Schlafen2 (Slfn2)	1.78 ± 0.22	2.35 ± 0.07
M57683	Platelet derived growth factor receptor, alpha	1.80 ± 1.34	1.55 ± 0.21
M62470	Thrombospondin 1	1.85 ± 0.24	2.10 ± 0.14
AJ009862	Transforming growth factor-beta 1	2.15 ± 0.87	3.95 ± 0.35
M26071	Coagulation factor III	2.28 ± 0.38	2.80 ± 0.14
L31958	pMAT1	2.93 ± 0.46	3.60 ± 0.14
AF065947	Small inducible cytokine A5	4.03 ± 0.80	3.40 ± 0.28
V00741	Epidermal growth factor	−3.03 ± 0.05	−5.00 ± 0.14
M17979	Epidermal growth factor binding protein type A	−2.68 ± 0.17	−3.20 ± 0.28
M17962	Epidermal growth factor binding protein type C	−2.55 ± 0.10	−2.75 ± 0.35
L12447	Insulin-like growth factor binding protein 5	−123 ± 0.05	−0.45 ± 0.07
X76066	Insulin like growth factor binding protein 4	−1.00 ± 0.08	−0.85 ± 0.07
U15012	Growth hormone receptor	−0.78 ± 0.17	−1.95 ± 0.21
M30641	Fibroblast growth factor 1	−0.58 ± 0.26	−1.15 ± 0.35

Affymetrix oligonucleotide gene expression analysis of obstructed kidneys ($N = 4$) compared to contralateral control kidneys ($N = 4$) at both day 4 and day 10 postobstruction. Numbers represent the mean signal log ratio, where 1 is equivalent to a twofold change in expression.

[a] Columns represent the mean of four comparisons ± standard deviation (SD) (the four comparisons are from straight and cross-comparisons of the duplicate chips at each time point).

[b] EST sequences which showed significant homology to the named genes by Blastn and Blastx searches on *http://www.ncbi.nlm.nih.gov/blast*

Table 2. Genes whose expression is altered at day 4 but not day 10 post unilateral ureteral obstruction (UUO)

GenBank ID	Gene family	Mean signal log ratio[a] Day 4 ± SD	Day 10 ± SD
	Cell growth and differentiation		
Y15163	Mrg1 protein	1.08 ± 0.17	NC
AF079528	IER5 (ler5) gene	1.28 ± 0.15	NC
U43084	Interferon-induced, tetratricopeptide repeats 1	1.35 ± 0.93	NC
U88908	Apoptosis inhibitor 1	3.05 ± 1.48	NC
M34896	Ecotropic viral integration site 2	3.15 ± 0.31	NC
	Cytokine and growth factor		
Al158810[b]	Interferon alpha induced 11.5kD protein	1.40 ± 0.32	NC
U56819	MCP-1 receptor mRNA	4.58 ± 0.17	NC

NC is no change (Affymetrix software).

Affymetrix oligonucleotide gene expression analysis of obstructed kidneys ($N = 4$) compared to contralateral control kidneys ($N = 4$) at both day 4 and day 10 postobstruction. Numbers represent the mean signal log ratio, where 1 is equivalent to a twofold change in expression.

[a]Columns represent the mean of four comparisons ± standard deviation (SD) (the four comparisons are from straight and cross-comparisons of the duplicate chips at each time point).

[b]EST sequences which showed significant homology to the named genes by Blastn and Blastx searches on *http://www.ncbi.nlm.nih.gov/blast*

Table 3. Genes whose expression is altered at day 10 but not day 4 post unilateral ureteral obstruction (UUO)

GenBank ID	Gene family	Mean signal log ratio[a] Day 4 ± SD	Day 10 ± SD
	Extracellular matrix and cytoskeletal		
X62622	Tissue inhibitor of metalloproteinase 2	NC	1.20 ± 0.14
X75285	Fibulin 2	NC	1.55 ± 0.07
Z38110	PMP22 peripheral myelin protein	NC	1.05 ± 0.07
X70853	BM-90/Fibulin	NC	1.05 ± 0.35
Y17808	A6 related protein	NC	1.50 ± 0.00
AB009993	Collagen a1(V)	NC	2.25 ± 0.78
M33960	Plasminogen activator inhibitor (PAI-1) mRNA	NC	2.25 ± 0.64
L36244	Matrix metalloproteinase 7	NC	5.70 ± 0.71
M82831	Macrophage metalloelastase	NC	3.45 ± 0.49
J04181	A-X actin mRNA	NC	−1.90 ± 1.41
	Cell growth and differentiation		
Y09864	Type I interferon receptor, IFNaR2b	NC	1.30 ± 0.14
Y13089	Caspase-11	NC	3.45 ± 1.77
	Cytokine and growth factor		
X81580	Insulin-like growth factor binding protein 2	NC	1.00 ± 0.28
D25540	TGF-beta type I receptor	NC	1.45 ± 0.21
M64849	Platelet derived growth factor, B polypeptide	NC	1.60 ± 0.28
AF004874	Latent TGF beta binding protein 2	NC	1.35 ± 0.21
D16250	BMP2 and BMP4 receptor	NC	1.55 ± 0.35
M21952	Macrophage colony-stimulating factor (4 kb)	NC	1.80 ± 0.71
U27267	Small inducible cytokine B subfamily, member 5	NC	3.45 ± 1.06
AB023418	Monocyte chemoattractant protein-2 precursor	NC	4.25 ± 0.07

NC is no change (Affymetrix software).

Affymetrix oligonucleotide gene expression analysis of obstructed kidneys ($N = 4$) compared to contralateral control kidneys ($N = 4$) at both day 4 and day 10 postobstruction. Numbers represent the mean signal log ratio, where 1 is equivalent to a twofold change in expression.

[a]Columns represent the mean of four comparisons ± standard deviation (SD) (the four comparisons are from straight and cross-comparisons of the duplicate chips at each time point).

previously to be down-regulated immediately after UUO and increased from day 5 onward [10]. This finding highlights the usefulness of our technique in dissecting the global gene expression changes occurring during progression of tubulointerstitial fibrosis.

To validate our model and to verify the expression patterns obtained from the microarray screen, we investigated the expression of five genes: TGF-β1, collagen type I α1, EGF, transgelin, and fisp-12/CTGF, using semiquantitative RT-PCR and quantitative real-time PCR. Since the association of TGF-β1 and collagen Iα1 with tubulointerstitial fibrosis has been extensively documented, we validated our system by monitoring the expression of these genes. Up-regulation of TGF-β1 was determined to be 2.15 ± 0.87 (day 4) and 3.95 ± 0.35 (day 10) (signal log ratio ± SD) by microarray analysis (Table 1) and was assessed at 4.8- and 2.6-fold compared to respective contralateral levels at days 4 and 10 post-UUO, respectively, using real-time PCR (Fig. 1A). Collagen Iα1 mRNA levels were also up-regulated, 1.93 ± 0.1 (day 4) and 2.10 ± 0.28 (day 10) (signal to log ratio ± SD) and this up-regulation was confirmed by RT-PCR analysis (Fig. 1B) with relative mRNA levels increasing from 0.22 ± 0.01 to 1.35 ± 0.10 at day 4 ($P < 0.01$) and from 0.29 ± 0.08 to 3.4 ± 0.19 at day 10 post-UUO ($P < 0.001$) (Fig. 1B and C). EGF was down-regulated −3.03 ± 0.05 by day 4 and −5.00 ± 0.14 by day 10 (signal log ratio) and the relative mRNA levels as determined by RT-PCR analysis decreased from 2.0 ± 0.53 to 0.63 ± 0.09 at day 4 and from 3.32 ± 0.44 to 0.23 ± 0.05 by day 10 ($P < 0.001$) (Fig. 1B and C). Transgelin was up-regulated by 1.6 ± 0.12 and 1.75 ± 0.21 (signal log ratio ± SD) at days 4 and 10 post-UUO, respectively. Again this regulation was confirmed by RT-PCR with the relative mRNA levels increasing from 0.20 ± 0.01 to 1.61 ± 0.4 ($P < 0.01$) at day 4 and from 0.74 ± 0.03 to 3.61 ± 0.33 at day 10 ($P < 0.001$) (Fig. 1B and C).

Fisp-12 was up-regulated by 1.1 ± 0.24 (day 4) and 1.45 ± 0.07 (day 10) (signal log ratio ± SD) in the microarray analysis, by quantitative real-time PCR, the relative abundance of fisp-12 was calculated at 1.9- and 2.6-fold, respectively (Fig. 1A). RT-PCR analysis confirmed these findings with relative quantities detected at 0.97 ± 0.02 to 4.05 ± 0.11 ($P < 0.001$) at day 4 and from 1.57 ± 0.06 to 2.95 ± 0.12 at day 10 ($P < 0.01$) (Fig. 1B and C).

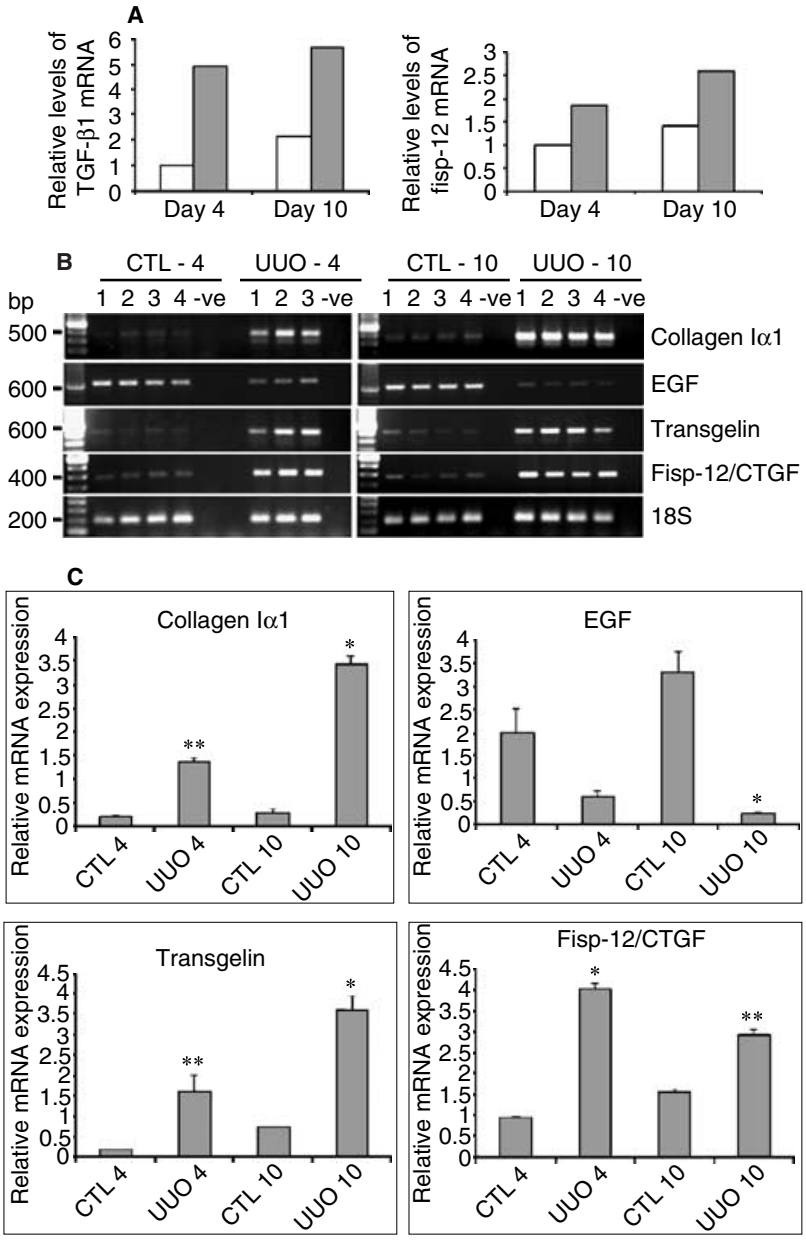

Fig. 1. Validation of oligonucleotide microarray analysis by quantitiative polymerase chain reaction (PCR) and reverse transcription (RT)-PCR highlighting the induction of fibroblast-inducible secreted protein (fisp-12), the murine homologue of human connective tissue growth factor (CTGF). (*A*) Quantitative real-time PCR for transforming growth factor-β1 (TGF-β1) and fisp-12 at days 4 and 10 postobstruction ($N = 4$, pooled mRNA) confirming the gene expression changes observed on the oligonucleotide microarray. Results are displayed as relative quantities normalized to respective 18S rRNA levels. Symbols are: (□) contralateral control kidney; (■) unilateral ureteral obstructed kidney. (*B*) RT-PCR of contralateral control (CTL) ($N = 4$ for day 4 and day 10) and unilateral ureteral obstructed (UUO) ($N = 3$ for day 4 and $N = 4$ for day 10) kidneys for genes identified in the microarray screen as differentially regulated in response to UUO. Negative RT-PCR reactions (-ve) were performed on RNA pooled for each time point and reverse transcribed in the absence of reverse trancriptase enzyme. (*C*) Densitometric analysis of the RT-PCR data from (B), each transcript is normalized to its respective 18S rRNA transcript level. Mean values ± SEM are shown. $^{*}P < 0.001$ and $^{**}P < 0.01$ compared to respective contralateral kidneys.

EMT of tubule epithelial cells by TGF-β 1 and EGF induces fisp-12, collagen XVIIIα 1, SSeCKS, and SPARC mRNA expression

Increased numbers of fibroblasts within the interstitial area are characteristic of tubulointerstitial fibrosis associated with ESRD [18]. TGF-β1 has been implicated in this process by stimulating EMT of tubule epithelial cells toward a fibroblast-like phenotype [18–20]. Stimulation of proximal tubular epithelial MCT cells with 3 ng/mL or 10 ng/mL TGF-β1 induced a significant increase in CTGF mRNA levels by 24 hours to 1.2-fold ($P < 0.05$) and 1.3-fold ($P < 0.001$), respectively, compared to vehicle-treated cells as assessed by quantitative real-time PCR (Fig. 2A).

To assess the influence of EMT on fisp-12 levels, we stimulated MCTs cells with 3 ng/mL TGF-β1 and 10 ng/mL EGF for 72 hours to induce EMT [19]. The combination of TGF-β1 and EGF has been reported to enhance the process of EMT in MCT cells [19], therefore we used this combination to maximize the number of transitioned cells. During this process, epithelial cells lose their cell-cell contacts, elongate to display a fibroblastic appearance (Fig. 2B), and express increased levels of fsp-1. Analysis of RT-PCR products, using densitometry, for fsp-1 mRNA confirmed the induction of this transcript from 1.00 ± 0.17 for vehicle-treated cells, relative to GAPDH levels, to 1.93 ± 0.21 for transitioned cells ($P < 0.005$) (Fig. 2C). Analysis of fisp-12

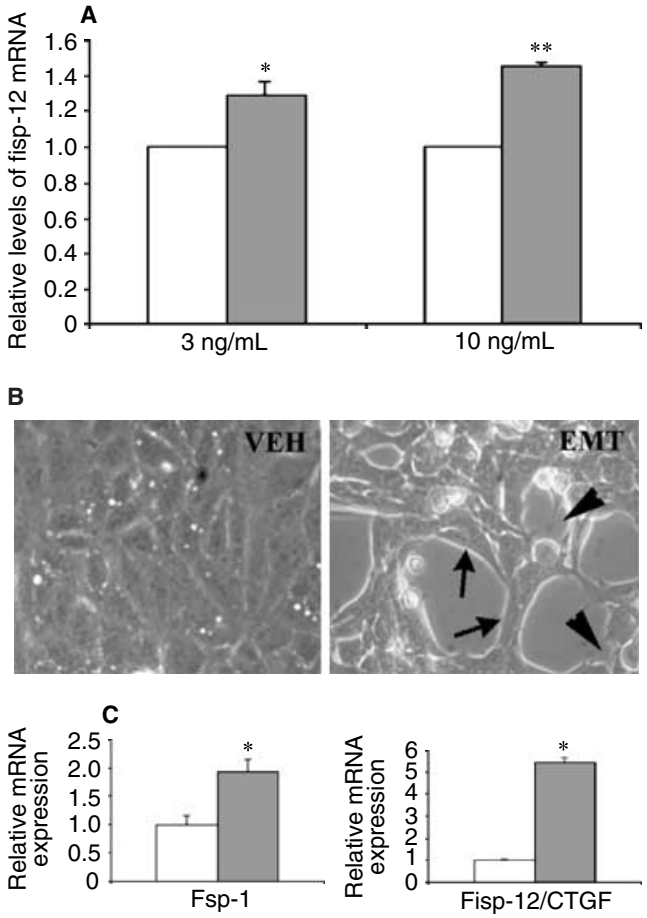

Fig. 2. Epithelial to mesenchymal transition (EMT) of tubular epithelial cells in vitro is associated with the induction of fibroblast-inducible secreted protein (fisp-12) expression. (*A*) Quantitative real-time polymerase chain reaction (PCR) detection of increased fisp-12 mRNA expression following exposure of MCT cells to 3 ng/mL and 10 ng/mL transforming growth factor-β1 (TGF-β1) for 24 hours in vitro ($N = 3$). $^{*}P < 0.05$; $^{**}P < 0.001$ vs. vehicle-treated cells. Symbols are: (□) vehicle-treated; (■) TGF-β1-treated. (*B*) Morphologic evidence of EMT following exposure of murine proximal tubular (MCT) cells to 3 ng/mL TGF-β1 and 10 ng/mL epidermal growth factor (EGF) for 72 hours (arrows show elongated cells, arrowheads show loss of cell to cell contacts) (magnification ×400). (*C*) Relative abundance of fibroblast specific protein-1 (fsp-1), and fisp-12 mRNA in vehicle-treated (□) and EMT-stimulated (■) MCT cells. Results are derived from densitometric analysis of reverse transcription (RT)-PCR products from three independent experiments, each performed in triplicate, normalized to respective glyceraldehyde-3-phosphate dehydrogenase (GAPDH) housekeeping gene levels. $^{*}P < 0.005$ vs. vehicle-treated cells.

in vehicle-treated and transitioned MCTs (normalized to their respective GAPDH levels) revealed a significant increase in the mRNA level of this transcript during transition, from 1.00 ± 0.05 to 5.47 ± 0.23 ($P < 0.005$) (Fig. 2C).

We analyzed three other putative profibrogenic genes, which were identified in the UUO microarray screen, during transition of tubule epithelial cells. Collagen XVIIIα1, SPARC, and SSeCKS were up-regulated at both days 4 and 10 post-UUO (Table 1), these changes in gene expression were confirmed by RT-PCR (Fig. 3A). Collagen XVIIIα1 and SSeCKS mRNA levels were nondetectable in contralateral kidneys but were significantly increased in the obstructed kidney ($P < 0.05$) (Fig. 3B). SPARC mRNA levels were slightly elevated above contralateral at day 4 but were significantly increased by day 10 from 1.26 ± 0.46 to 2.66 ± 0.27 ($P < 0.05$) (Fig. 3C).

Transcript levels for all three genes were monitored during transition of MCT cells. mRNA levels for collagen XVIIIα1, SPARC, and SSeCKS were significantly induced in transitioned cells (Fig. 3C and D), from 0.74 ± 0.02 in vehicle-treated cells to 1.78 ± 0.27 ($P < 0.02$ compared to vehicle) for collagen XVIIIα1, from 1.05 ± 0.06 to 2.13 ± 0.49 ($P \leq 0.005$ compared to vehicle) for SPARC, and from 0.44 ± 0.08 to 2.29 ± 0.33 ($P \leq 0.005$) for SSeCKS.

DISCUSSION

In the current study, oligonucleotide microarray analysis of murine UUO kidneys led to the identification of changes in the expression of 1091 genes during progression to tubulointerstitial fibrosis. Functional classification revealed marked alterations in the expression of genes involved with extracellular matrix, cytoskeletal reorganisation, signaling pathways, and cell cycle progression and regulation. Initially in obstructed kidneys, there is an influx of mononuclear cells, which secrete cytokines and growth factors, which act on the renal interstitium to promote the development of fibrosis [22]. By analyzing gene expression at an early and a later time point, day 4 and day 10 postobstruction, we hoped to identify changes in gene expression, which reflect the temporal changes in the morphology of obstructed kidneys [13, 23]. Interestingly, we found that the majority of genes which displayed an alteration in expression level at day 4 were further altered by day 10, suggesting that persistent rather than transient changes in gene expression are important in the development of tubulointerstitial fibrosis.

Genes encoding extracellular matrix/cytoskeletal molecules underwent major transcriptional alterations during UUO, 64 genes were identified which were significantly up-regulated by days 4 and 10 post-UUO compared to the contralateral kidney reflecting the morphologic changes observed in fibrotic kidneys. Significantly increased transcript levels for these molecules, including collagens I, III, IV, V, VI, XV, XVIII, nidogen, tenascin C, and cadherin among others, were observed as early as 4 days after obstruction, highlighting the importance of differential regulation of these genes in the initial stages of fibrosis. Of note, transcript levels for collagens I and III showed greater increases than collagen IV, confirming previous findings for these molecules. Transcript levels for molecules which regulate the turnover of these extracellular matrix proteins were also differentially

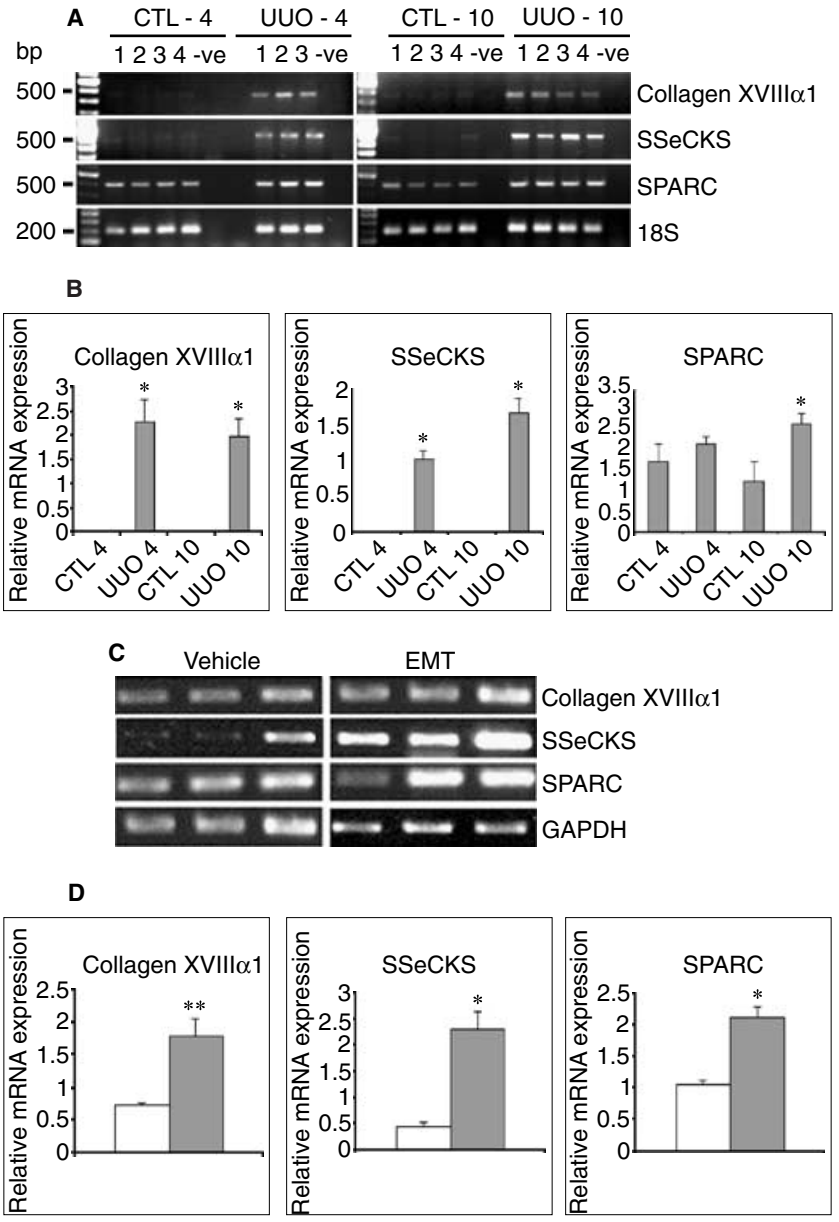

Fig. 3. mRNA levels for collagen XVIIIα 1, src-suppressed C-kinase substrate (SSeCKS), and secreted protein acidic and rich in cysteine (SPARC), are increased in response to unilateral ureteral obstruction (UUO) and during epithelial to mesenchymal transition (EMT) of tubular epithelial cells. (*A*) Reverse transcription-polymerase chain reaction (RT-PCR) analysis of contralateral control (CTL) ($N = 4$ for day 4 and day 10) and obstructed (UUO) ($N = 3$ for day 4 and $N = 4$ for day 10) kidneys at days 4 and 10 confirming the data obtained in the oligonucleotide microarray screen. (*B*) Densitometric analysis of the RT-PCR data in (A), each transcript is normalized to its respective 18S rRNA transcript level, mean values ± SEM are shown, $^{*}P < 0.05$. (*C*) RT-PCR analysis of mRNA transcripts for collagen XVIIIα1, SSeCKS, and SPARC in vehicle-treated and EMT-stimulated murine proximal tubular (MCT) cells. Three independent experiments were perfomed, each in triplicate. A representative experiment is shown. (*D*) Densitometric analysis of the RT-PCR products. Symbols are: (□) vehicle-treated; (■) EMT-stimulated. Results are derived from three independent experiments, each performed in triplicate, normalized to respective glyceraldehyde-3-phosphate dehydrogenase (GAPDH) housekeeping gene levels ($N = 3$). $^{*}P < 0.02$; $^{**}P \leq 0.005$.

regulated with tissue inhibitors of metalloproteinase (TIMP-3) down-regulated at both days 4 and 10 and TIMP-2 only showing up-regulation by day 10 and not by day 4. Interestingly, mRNA levels for matrix metalloproteinase (MMP-7) were not significantly changed during the early stages of renal fibrosis but were significantly increased by day 10 (Table 2). MMP-7 levels have been found to be increased in pulmonary fibrosis and mice deficient for MMP-7 were protected from bleomycin-induced pulmonary fibrosis [24]. These findings serve to validate our model and highlight the importance of differential gene expression which underlies the progression of tubulointerstitial fibrosis.

Another important gene family which showed marked alteration with UUO included transcripts encoding for molecules involved with cell cycle regulation, including cytokines and growth factors. As expected, EGF was down-regulated in response to UUO along with insulin-like growth factor binding proteins, this may result in an environment conducive to the loss of epithelial growth signals, leading to a reduction in epithelial cell survival and contributing to the loss of epithelial integrity.

Changes in tissue mRNA levels in vivo can reflect both changes in the transcriptome of resident tissue cells and the presence of infiltrating cells. Whereas the latter are relevant to studies pertaining to molecular diagnostics, they may confound interpretation of studies addressing the regulation of gene expression in resident cells. To circumvent this difficulty, we complemented our in vivo microarray analysis in the present study with assessment

of the expression of a cohort of potentially profibrogenic genes in vitro in response to TGF-β1 stimulation and subsequent EMT.

TGF-β1 is an important cytokine within the kidney and has been implicated in portraying a pathologic role in renal disease [25–27]. The pleiotropic actions of TGF-β1 in the kidney include suppression of mononuclear cell proliferation, induction of other cytokines [25], and induction of EMT, limiting its attractiveness as a therapeutic target. Blockade of fisp-12/CTGF may offer an alternative therapeutic strategy. TGF-β1 has been shown to induce EMT, which results in alterations of cell morphology to a more "fibroblast-like" phenotype and functional profile [19, 28]. EMT is becoming more widely associated with tubulointerstitial fibrosis and has been reported in a number of renal diseases, which include fibrotic lesions associated with ESRD. EMT occurs in response to cytokines such as TGF-β1, EGF, fibroblast growth factor 2 (FGF-2), interleukin-1 (IL-1), and combinations of cytokines can induce EMT to a greater extent [18, 29, 30]. Here we describe the induction of fisp-12, the murine homologue of CTGF, during UUO showing that this gene functions during fibrosis. We observed that TGF-β1 stimulation alone induced a transient twofold increase in CTGF mRNA levels which declines after 24 hours of treatment (data not shown). However, we observed a fivefold increase in CTGF mRNA levels when MCT cells were induced to undergo EMT, revealing that a sustained increase in CTGF production occurs during the cytoskeletal remodeling triggered during EMT. This suggests that CTGF may play a role in the morphologic changes observed during EMT and therefore warrants further investigation. Since remodeling of tubular epithelium is a critical factor in tissue fibrosis leading to significant loss of renal function, this observation for CTGF may uncover a novel mechanism for controlling tubule integrity during renal fibrosis.

In this report, we have demonstrated that fisp-12 expression is promoted by TGF-β1 in renal proximal tubular cells and is induced during the process of EMT in response to this cytokine. Recently, CTGF has been shown to increase the production of collagen I in renal fibroblasts showing that it too can induce alterations to the extracellular matrix and contribute to the overall change in extracellular matrix composition as seen with tubulointerstitial fibrosis [15].

Among the genes up-regulated in UUO reported in this paper were collagen XVIIIα1, SPARC, and SSeCKS. We focused on these genes since we believe they have a potential role in the regulation of cell morphology, the alteration of which underlies the tubular changes observed in UUO. Up-regulation of these genes was confirmed within UUO and furthermore we have demonstrated their up-regulation during EMT. Collagen XVIIIα1, also known as endostatin; an angiogenesis inhibitor, has been demonstrated to have a pathogenic role in chronic liver fibrosis [32]. It is expressed in mouse basement membranes, vascular smooth muscle cells and epithelia and displays high expression within the liver. Activated stellate cells and myofibroblasts in human fibrotic livers were shown to increase their levels of collagen XVIIIα1, resulting in its association with basement membrane remodeling [33]. This correlates with our finding of increased expression of collagen XVIIIα1 in epithelial cells undergoing EMT, which display a stellate, fibroblast-phenotype.

SPARC is a secreted glycoprotein that affects cellular interactions with matrix proteins [34]. It has been implicated in extracellular matrix deposition and has been shown to bind collagen types I, III, IV, V, and VIII [35], all of which are up-regulated during UUO. SPARC augments the production of PAI-1 and the MMPs: collagenase, gelatinase, and stromolysin [36]. Its expression is increased by TGF-β1, IL-1, and colony stimulating factor 1 (CSF-1), and has been detected in interstitial α-smooth muscle actin(α-SMA)-positive fibroblasts [35]. SPARC colocalizes with collagen type I–expressing cells in experimental models in which tubulointerstitial fibrosis occurs such as passive Heymann nephritis (PHN), cyclosporine A nephropathy, remnant kidney, and angiotensin II infusion model [34]. SPARC has been shown to inhibit proliferation of endothelial cells, fibroblasts, and smooth muscle cells and its expression correlates with the resolution of interstitial cell proliferation at day 15 of PHN [34]. In PHN, glomerular epithelial cells and spindle-shaped interstitial cells, in areas of extracellular matrix expansion, were found to express SPARC.

SSeCKS was originally isolated as an src-suppressed negative mitogenic regulator in fibroblasts [37]. SSeCKS associates with cyclin D1 and sequesters it in the cytoplasm, inhibiting its translocation to the nucleus. In response to mitogenic growth factors, SSeCKS is rapidly phosphorylated by extracellular signal-regulated protein kinase (ERK-2), translocates to the perinucleus, loses its binding capacity for cyclin D1, which enables entry of cyclin D1 to the nucleus and the initiation of subsequent molecular events for the progression to S phase and cell proliferation [38]. In this manner, SSeCKS acts as a scaffolding protein linking signals between extracellular mitogens and downstream ERK-kinase signaling pathways such as protein kinase A (PKA) and protein kinase C (PKC). Expression of SSeCKS was abundant in human and rodent mesangial cells and glomerular parietal cells and was reported as undetectable in renal tubular epithelia [39]. This was surprising as we were able to detect SSeCKS mRNA in renal proximal tubule epithelial cells and found an increase in mRNA levels in cells undergoing EMT. It has been suggested that SSeCKS functions to maintain an elongated cell phenotype with stellate projections [39] and this would correspond to

our finding of increased SSeCKS mRNA in tubule epithelial cells undergoing transition, which display a stellate fibroblast phenotype. Our findings suggest a role for SSeCKS as a downstream mediator of TGF-β1–controlled actin-based cytoskeletal architecture.

A recent paper by Zavadil et al [31] describes the molecular alterations induced by TGF-β1 on human keratinocytes. Comparison of the genes identified in the TGF-β1 microarray analysis yields numerous similarities to the gene expression changes identified with our microarray data published here. Extracellular matrix–related molecules, which were positively regulated by TGF-β1 treatment, including transgelin, tenascin C, laminin, tubulin, and MMP-14, also displayed up-regulation in our microarray screen. TIMP-3 was down-regulated by TGF-β1 treatment and we also observed down-regulation of this molecule during UUO. This further highlights the important role that TGF-β1 plays in renal fibrosis and strengthens the requirement for the identification of a molecular target that mediates the fibrogenic effects of TGF-β1. We propose that CTGF, SPARC, SSeCKS, and collagen XVIIIα1 may represent such therapeutic targets.

Zavadil et al [31] conclude that TGF-β1 regulates (*1*) defined functional classes of molecules involved in epithelial plasticity and in the differentiation of transitional progenitor cells and (*2*) cohorts of genes involved in remodeling of the actin cytoskeleton and actin stress fiber formation. We conclude that genes involved in transition of one cell phenotype to another are important during the progression of tubulointerstitial fibrosis and that alterations in the expression of genes controlling these phenotypic changes is critical to the development of a fibrotic environment.

CONCLUSION

We report alterations of gene expression during the development of tubulointerstitial fibrosis. EMT results in the up-regulation of a number of genes whose mRNA levels are also increased during UUO, further highlighting the potential importance of this process during the development of fibrosis within the interstitium. Prominent among these molecules were several profibrogenic molecules, including fisp-12, collagen XVIIIα1, SSeCKS, and SPARC. The further delineation of the transcriptomic events underpinning renal fibrosis and of the molecular and signaling pathways that regulate these events should help unravel the complex mechanisms of tubulointerstitial scarring and suggest new approaches to the treatment of progressive renal disease.

ACKNOWLEDGMENTS

D.H. was supported by a Conway Institute Postdoctoral Fellowship and C.G. and H.R.B. are recipients of funding from the Health Research Board and the Irish Government Programme for Research in Third Level Institutes.

Reprint requests to Catherine Godson, Department of Medicine and Therapeutics, Conway Institute University College Dublin, Belfield, Dublin 4, Ireland.
E-mail: catherine.godson@ucd.ie

REFERENCES

1. D'Amico G, Ferrario F, Rastaldi MP: Tubulointerstitial damage in glomerular disease: Its role in the progression of renal damage. *Am J Kidney Dis* 26:124–132, 1995
2. Bohle A, Muller GA, Wehrmann M, *et al*: Pathogenesis of chronic renal failure in the primary glomerulopathies, renal vasculopathies, and chronic interstitial nephritides. *Kidney Int* 49(Suppl 54): S2–S9, 1996
3. Klahr S: New insights into the consequences and mechanisms of renal impairment in obstructive nephropathy. *Am J Kidney Dis* 18:689–699, 1991
4. Truong LD, Petrusevska G, Yang G, *et al*: Cell apoptosis and proliferation in experimental chronic obstructive uropathy. *Kidney Int* 50:200–207, 1996
5. Kaneto H, Morrissey J, Klahr S: Increased expression of TGF-beta 1 mRNA in the obstructed kidney of rats with unilateral ureteral ligation. *Kidney Int* 44:313–321, 1993
6. Ricardo SD, Levinson ME, DeJoseph MR, Diamond JR: Expression of adhesion molecules in rat renal cortex during experimental hydronephrosis. *Kidney Int* 50:2002–2010, 1996
7. Cheng QL, Chen XM, Li F, *et al*: Effects of ICAM-1 antisense oligonucleotide on the tubulointerstitium in mice with unilateral ureteral obstruction. *Kidney Int* 57:183–190, 2000
8. Moriyama T, Kawada N, Ando A, *et al*: Up-regulation of HSP47 in the mouse kidneys with unilateral ureteral obstruction. *Kidney Int* 54:110–119, 1998
9. Terada Y, Hanada S, Nakao A, *et al*: Gene transfer of Smad7 using electroporation of adenovirus prevents renal fibrosis in post-obstructed kidney. *Kidney Int* 61(Suppl 81): S94–S98, 2002
10. Duymelinck C, Dauwe SE, de Greef KE, *et al*: TIMP-1 gene expression and PAI-1 antigen after UUO in adult male rat. *Kidney Int* 58:1186–1201, 2000
11. Chevalier RL, Thornhill BA, Chang AY: Unilateral ureteral obstruction in neonatal rats leads to renal insufficiency in adulthood. *Kidney Int* 58:1987–1995, 2000
12. Klahr S, Purkerson ML: The pathophysiology of obstructive nephropathy: The role of vasoactive compounds in the hemodynamic and structural abnormalities of the obstructed kidney. *Am J Kidney Dis* 23:219–233, 1994
13. Vielhauer V, Anders H-J, Mack M, *et al*: Obstructive nephropathy in the mouse: Progressive fibrosis correlates with tubulointerstitial chemokine expression and accumulation of CC chemokine receptor 2- and 5-positive leukocytes. *J Am Soc Nephrol* 12:1173–1187, 2001
14. Gupta S, Clarkson MR, Duggan J, Brady HR: Connective tissue growth factor: Potential role in glomerulosclerosis and tubulointerstitial fibrosis. *Kidney Int* 58:1389–1399, 2000
15. Yokoi H, Mukoyama M, Sugawara A, *et al*: Role of connective tissue growth factor in fibronectin expression and tubulointerstitial fibrosis. *Am J Physiol Renal Physiol* 282:F933–F942, 2002
16. Iwano M, Plieth D, Danoff TM, *et al*: Evidence that fibroblasts derive from epithelium during tissue fibrosis. *J Clin Invest* 110:341–350, 2002
17. Abreu JG, Ketpura NI, Reversade B, De Robertis EM: Connective-tissue growth factor (CTGF) modulates cell signalling by BMP and TGF-beta. *Nat Cell Biol* 4:599–604, 2002
18. Okada H, Danoff TM, Kalluri R, Neilson EG: Early role of FSP1 in epithelial-mesenchymal transformation. *Am J Physiol* 42:F563–F574, 1997
19. Strutz F, Okada H, Lo CW, *et al*: Identification and characterisation of a fibroblast marker: FSP1. *J Cell Biol* 130:393–405, 1995

20. Strutz F, Muller GA: Transition comes of age. *Nephrol Dial Transplant* 15:1729–1731, 2000
21. Haverty TP, Kelly CJ, Hines WH, *et al*: Characterisation of a renal tubular epithelial cell line which secretes the autologous target antigen of autoimmune experimental interstitial nephritis. *J Cell Biol* 107:1359–1368, 1988
22. Schreiner GF, Harris KPG, Purkerson ML, Klahr S: Immunological aspects of acute ureteral obstruction: Immune cell infiltrate in the kidney. *Kidney Int* 34:487–493, 1988
23. Nagle RB, Bulger RE, Cutler RE, *et al*: Unilateral obstructive nephropathy in the rabbit: Early morphologic, physiologic and histochemical changes. *Lab Invest* 28:456–467, 1973
24. Zuo F, Kaminski N, Eugui E, *et al*: Gene expression analysis reveals matrilysin as a key regulator of pulmonary fibrosis in mice and humans. *PNAS* 99:6292–6297, 2002
25. Kettler M, Noble NA, Border WA: Increased expression of transforming growth factor-β in renal disease. *Curr Opin Nephrol Hyperten* 3:446–452, 1994
26. Blobe GC, Schieman WP, Lodish HF: Role of transforming growth factor β in human disease. *N Engl J Med* 342:1350–1358, 2000
27. Isaka Y, Tsujie M, Ando Y, *et al*: Transforming growth factor-β1 antisense oligodeoxynucleotides block tubulointerstitial fibrosis in unilateral ureteral obstruction. *Kidney Int* 58:1885–1892, 2000
28. Fan JM, Ng YY, Hill PA, *et al*: Transforming growth factor-beta regulates tubular epithelial-myofibroblast transition in vitro. *Kidney Int* 56:1455–1467, 1999
29. Fan JM, Huang XR, Ng YY, *et al*: Interleukin-1 induces tubular epithelial-myofibroblast transition through a transforming growth factor-beta 1-dependent mechanism in vitro. *Am J Kidney Dis* 37:820–831, 2001
30. Strutz F, Zeilsberg M, Ziyadeh FN, *et al*: Role of basic fibroblast growth factor-2 in epithelial-mesenchymal transformation. *Kidney Int* 61:1714–1728, 2002
31. Zavadil J, Bitzer M, Liang D, *et al*: Genetic programs of epithelial cell plasticity directed by transforming growth factor-β. *PNAS* 98:6686–6691, 2001
32. Jia JD, Bauer M, Sadlaczec N, *et al*: Modulation of collagen XVIII/endostatin expression in lobular and biliary liver fibrogenesis. *J Hepatol* 35:386–391, 2001
33. Musso O, Rehn N, Saarela J, *et al*: Collagen XVIII is localised in sinusoids and basement membrane zones and expressed by hepatocytes and activated stellate cells in fibrotic human liver. *Hepatology* 28:98–107, 1998
34. Pichler RN, Hugo C, Shankland SJ, *et al*: SPARC is expressed in renal interstitial fibrosis and in renal vascular injury. *Kidney Int* 50:1978–1989, 1996
35. Lane TF, Sage EH: The biology of SPARC a protein that modulates cell-matrix interactions. *FASEB J* 8:163–173, 1994
36. Tremble PM, Lane TF, Sage EH, Werb Z: SPARC, a secreted protein associated with morphogenesis and tissue remodelling, induces expression of metalloproteinases in fibroblasts through a novel extracellular matrix-dependent pathway. *J Cell Biol* 121:1433–1444, 1993
37. Lin X, Nelson PJ, Frankfort B, *et al*: Isolation and characterisation of a novel mitogenic regulatory gene, 322, which is transcriptionally suppressed in cells transformed by src and ras. *Mol Cell Biol* 15:2754–2762, 1995
38. Lin X, Nelson P, Gelman IH: SSeCKS: A major protein kinase C substrate with tumour suppressor activity, regulates G_1-S progression by controlling the expression and cellular compartmentalisation of cyclin D. *Mol Cell Biol* 20:7259–7272, 2000
39. Nelson PJ, Moissoglu K, Vargas J, *et al*: Involvement of the protein kinase X substrate, SSeCKS, in the actin-based stellate morphology of mesangial cells. *J Cell Sci* 112:361–370, 1999